

**Exploratory Clinical Investigation of (4S)-4-(3-<sup>18</sup>F-Fluoropropyl)-L-Glutamate  
Positron Emission Tomography of Inflammatory and Infectious Lesions**

Sun Young Chae<sup>1</sup>, Chang-Min Choi<sup>2</sup>, Tae Sun Shim<sup>2</sup>, Yangsoon Park<sup>3</sup>, Chan-Sik Park<sup>3</sup>,  
Hyo Sang Lee<sup>1</sup>, Sang Ju Lee<sup>1</sup>, Seung Jun Oh<sup>1</sup>, Seog-Young Kim<sup>4</sup>, Sora Baek<sup>5</sup>,  
Norman Koglin<sup>6</sup>, Andrew W. Stephens<sup>6</sup>, Ludger M. Dinkelborg<sup>6</sup> and Dae Hyuk Moon<sup>1</sup>

Departments of <sup>1</sup>Nuclear Medicine, <sup>2</sup>Pulmonology, and <sup>3</sup>Pathology, and <sup>4</sup>Institute for  
Innovative Cancer Research, Asan Medical Center, University of Ulsan College of  
Medicine, Seoul, Republic of Korea; <sup>5</sup>Department of Nuclear Medicine, Kangdong  
Sacred Heart Hospital, Hallym University College of Medicine, Seoul, Republic of  
Korea; and <sup>6</sup>Piramal Imaging, Berlin, Germany

**Corresponding author:** Dae Hyuk Moon, M.D., Ph.D.,

Department of Nuclear Medicine, Asan Medical Center, University of Ulsan College of  
Medicine, 88, Olympic-ro 43-gil, Songpa-gu, Seoul 138-736, Korea

Tel: 82-2-3010-4592, Fax: 82-2-3010-4588, E-mail: dhmoon@amc.seoul.kr

**First author:** Sun Young Chae, M.D. (not under training)

Department of Nuclear Medicine, Asan Medical Center, University of Ulsan College of  
Medicine, 88, Olympic-ro 43-gil, Songpa-gu, Seoul 138-736, Korea

Tel: 82-2-3010-5448, Fax: 82-2-3010-4588, E-mail: sychae@amc.seoul.kr

Total word count of the manuscript: 2500

Financial support: This study was sponsored and financially supported by Bayer  
Pharma AG/Piramal Imaging GmbH, Berlin, Germany

Short running title: FSPG PET in inflammation

## ABSTRACT

We explored system  $x_c^-$  transporter activity and the detection of inflammatory/infectious lesions using (4S)-4-(3- $^{18}\text{F}$ -fluoropropyl)-L-glutamate ( $^{18}\text{F}$ -FSPG) positron emission tomography (PET). **Methods:** In ten patients with various inflammatory/infectious diseases, as many as five of the largest lesions were selected as reference lesions.  $^{18}\text{F}$ -FSPG images were assessed visually and quantitatively. Expression levels of xCT, CD44, and surface markers of inflammatory cells were evaluated by immunohistochemistry. **Results:**  $^{18}\text{F}$ -FSPG PET detected all reference lesions.  $^{18}\text{F}$ -FSPG uptake in sarcoidosis was significantly higher than that in non-sarcoidosis. The lesion-to-blood pool standardized uptake value (SUV) ratio of  $^{18}\text{F}$ -FSPG was comparable to that of  $^{18}\text{F}$ -fluorodeoxyglucose in sarcoidosis. In non-sarcoidosis, however, it was significantly lower. In five with available tissue samples, the maximum SUV of  $^{18}\text{F}$ -FSPG and CD163 were negatively correlated ( $\rho = -0,872$ ,  $P = 0.054$ ). **Conclusion:**  $^{18}\text{F}$ -FSPG PET may detect inflammatory lesions where activated macrophages/monocytes are present such as in sarcoidosis.

**Key words:** glutamate;  $x_c^-$  transporter; positron emission tomography; inflammation; infection

The system  $x_c^-$  is composed of xCT and 4F2hc, mediating cellular cystine uptake for glutathione synthesis to protect cells from oxidative stress (1). Several lines of evidence suggest that system  $x_c^-$  may play a role in the innate and adaptive immune system. Upregulation of system  $x_c^-$  expression was observed in activated macrophages and granulocytes (2,3). Induction of system  $x_c^-$  might be an autoprotective mechanism from the high levels of released reactive oxygen species (4). Activation of T-lymphocytes has been reported to involve expression of system  $x_c^-$  in antigen presenting cells (5,6). Upregulation of xCT occurs during activation and differentiation of B lymphocyte (7). On the other hand, very low or no expression of xCT was detected in peripheral leukocytes, thymus, spleen, and lymph nodes in human (8). These results suggest that system  $x_c^-$  is a key player in the active phase of inflammation.

(4S)-4-(3- $^{18}\text{F}$ -Fluoropropyl)-L-Glutamate ( $^{18}\text{F}$ -FSPG) is a new  $^{18}\text{F}$ -labeled L-glutamate derivative that is specifically taken up by the system  $x_c^-$  as previously demonstrated in tumor models and cancer patients (9,10). The primary objective was to explore the detection of inflammatory lesions as the result of infectious and noninfectious cause by  $^{18}\text{F}$ -FSPG PET. The secondary objectives were to perform quantitative analyses of  $^{18}\text{F}$ -FSPG uptake and compare the results obtained with those obtained using  $^{18}\text{F}$ -FDG. In addition, we evaluated the expression of xCT, CD44 and surface markers of inflammatory cells by immunohistochemistry to explore their correlations with  $^{18}\text{F}$ -FSPG uptake.

## **MATERIALS AND METHODS**

### **Study Design**

The study was conducted as an open-label, nonrandomized, single-dose explorative

study. The study protocol was approved by both the Institutional Review Board and the Korea Food and Drug Administration. All patients provided written informed consent before participation in the study.

### **Radiopharmaceutical Preparation**

Radiolabeling of  $^{18}\text{F}$ -FSPG was conducted as described previously (9). The specific activity of  $^{18}\text{F}$ -FSPG formulated for intravenous administration was  $74.4 \pm 59.6$  GBq/ $\mu\text{mol}$  (range, 35.0–235.6 GBq/ $\mu\text{mol}$ ), and the radiochemical purity was  $91.6\% \pm 1.5\%$  (range, 90.1%–94.4%).

### **Patients**

Patients were enrolled if they had inflammatory/infectious diseases with strong clinical or laboratory evidence of inflammatory/infectious focus/foci in defined anatomical regions preferably visible on  $^{18}\text{F}$ -FDG PET/CT scans. Full eligibility criteria are shown in Supplemental Appendix.

### **PET/CT Procedure**

$^{18}\text{F}$ -FDG and  $^{18}\text{F}$ -FSPG PET/CT (10) were performed as previously described using the same PET/CT scanner (Biograph True Point 40; Siemens).  $^{18}\text{F}$ -FSPG PET/CT examination was conducted during three time windows (0–45 min, 60–75 min, and 105–120 min) following injection of  $300 \pm 10$  MBq of  $^{18}\text{F}$ -FSPG.

### **Image Analysis**

The PET/CT images were assessed visually and quantitatively by two board-certified nuclear medicine physicians as previously reported (10). Mean standardized uptake

values (SUVmean) were obtained to generate a time activity profile of  $^{18}\text{F}$ -FSPG uptake. The PET/CT images at 60 minutes post-injection were used for visual and quantitative analysis. The largest inflammatory/infectious lesion was chosen as the representative lesion for patient-based analysis. As many as five of the largest lesions were selected as reference lesions. The SUV ratio (SUVR) was calculated by dividing the maximum SUV (SUVmax) of the reference lesion by the SUVmean of blood pool activity.

### **Immunohistochemical staining of xCT, CD44, and surface markers of inflammatory cells**

Immunohistochemical (IHC) staining methods are shown in Supplemental Appendix.

### **Statistical Analysis**

Comparison was conducted using the Mann-Whitney  $U$  test, Fisher's exact test, and Spearman rank correlation coefficients ( $\rho$ ) using the IBM SPSS Statistics Version 21 for Windows (SPSS, Inc., IBM Company).

## **RESULTS**

### **Patients and $^{18}\text{F}$ -FSPG PET/CT Procedure**

Five men and five women were enrolled (ages 42–66 years). All but two patients underwent  $^{18}\text{F}$ -FDG PET/CT. The mean time interval between  $^{18}\text{F}$ -FDG and  $^{18}\text{F}$ -FSPG PET/CT was  $2.0 \pm 1.8$  days (range, 1–6 days). The baseline characteristics are summarized in Supplemental Table 1. Twenty-four reference lesions in ten patients were selected (lung, 17; lymph node, 7).

### **Biodistribution of <sup>18</sup>F-FSPG**

SUVmean of normal tissues and inflammatory/infectious lesions are summarized in Supplemental Fig. 1. The kidney and pancreas showed high uptake, whereas the spleen exhibited low uptake. There was no or negligible uptake in the brain, myocardium, muscle, intestinal track, and bone.

### **<sup>18</sup>F-FSPG Uptake in Inflammatory/Infectious Lesions**

The patient-based (10/10, 7 major and 3 minor accumulations) and lesion-based (24/24, 15 major and 7 minor accumulations) detection rates by visual assessment were 100%.

All sarcoid reference lesions (10/10) showed major uptake (Fig. 1), while only 36% (5/14) of non-sarcoid lesions had the same uptake (Supplemental Fig. 2,  $P = 0.002$ ). SUVmax values were significantly higher in sarcoidosis than those in non-sarcoidosis as were the SUVR values ( $P < 0.001$ , Fig. 2). SUVmax and SUVR of <sup>18</sup>F-FDG in sarcoidosis were also significantly higher than those in non-sarcoidosis ( $P = 0.001$  and  $P = 0.006$ , respectively, Fig. 2).

The visually assessed intensity of <sup>18</sup>F-FSPG accumulation in reference lesions was the same as that of <sup>18</sup>F-FDG (100%, 10/10) in sarcoidosis, whereas 92% (11/12) of the lesions in non-sarcoidosis had lower <sup>18</sup>F-FSPG accumulation (Supplemental Fig. 3). Quantitative analysis showed that SUVR of <sup>18</sup>F-FSPG in sarcoid lesions at 60 minutes post-injection was comparable to that of <sup>18</sup>F-FDG ( $P = 0.481$ , Fig. 2A) although the SUVmax values of <sup>18</sup>F-FSPG were significantly lower than those of <sup>18</sup>F-FDG ( $P < 0.001$ , Fig. 2B). In non-sarcoidosis, SUVmax and SUVR of <sup>18</sup>F-FSPG were significantly lower than those of <sup>18</sup>F-FDG ( $P < 0.05$ , Fig. 2).

### **<sup>18</sup>F-FSPG Uptake and Correlation with IHC Staining**

A total of eight patients underwent core needle biopsy, but sufficient tissue sample was available from only five patients. The results of IHC analysis are shown in Supplemental Table 2. All five patients showed positive xCT expression in  $\geq 50\%$  of inflammatory cells. Histiocytes and plasma cells showed positive xCT staining (Fig. 1, Supplemental Fig. 2 and Supplemental Fig. 4). In two of three patients with major accumulation, the proportion of CD44 expression was  $\geq 80\%$  (Fig. 1 and Supplemental Fig. 4), while two patients with minor uptake showed  $\leq 30\%$  positive cells (Supplemental Fig. 2). The proportion of IHC staining of xCT correlated significantly with that of CD68 ( $\rho = 0.9$ ,  $P = 0.037$ ). The SUVmax of <sup>18</sup>F-FSPG was negatively correlated with CD163 positive cells with borderline significance ( $\rho = -0.872$ ,  $P = 0.054$ ). However, no correlation was found with other surface markers of inflammatory cells.

### **DISCUSSION**

We found that <sup>18</sup>F-FSPG uptake in patients with sarcoidosis was significantly higher than in patients with non-sarcoidosis. Inflammatory mechanisms of sarcoidosis include activation of macrophages and dendritic cells (11). Of note, two patients with sarcoidosis had had elevated serum ACE and systemic symptoms. On the other hand, patients with non-sarcoidosis presented with radiological abnormalities without systemic symptoms. The inclusion of non-sarcoidosis patients was influenced by other diagnostic imaging studies that may have selected patients with a less active disease process. This selection strategy may have led to spectrum bias in this study. This explanation is supported by higher <sup>18</sup>F-FDG uptake in patients with sarcoidosis than in patients with non-sarcoidosis.

Our results showed that the proportion of positive xCT staining cells correlated significantly with that of CD68 positive cells. However, the SUVmax of  $^{18}\text{F}$ -FSPG did not correlate with xCT, CD44, or CD68 expression. The small number of patients and the limited amount of tissue available for IHC staining may have prevented us from obtaining a positive correlation. By contrast, previous examinations in tissue samples from tumor patients showed a correlation, suggesting that different and/or additional components contribute to uptake and retention in tumors and inflammatory tissue. The lack of correlation between  $^{18}\text{F}$ -FSPG and xCT or CD44 might also be because xCT expression has an additional role to play in remitting the chronic inflammatory response (4). In a mouse model of chronic inflammation induced by 3-methylcholanthrene, xCT mRNA was significantly up-regulated, whereas xCT expression contributed to the termination of inflammation (3,4). In lipopolysaccharide-induced inflammation, a very high initial rate of cystine uptake in macrophages was followed by a decrease in uptake at a later phase of inflammation (2). Finally, the regulation of CD44 on system  $\text{x}_c^-$  might be different in inflammation compared to that in cancer. There is a need for more studies on the regulation of system  $\text{x}_c^-$  activity in inflammation.

SUVmax of  $^{18}\text{F}$ -FSPG was negatively correlated with CD163 positive staining, which is predominantly associated with M2 macrophages (12). In Patient 5 with sarcoidosis (Fig. 1), only 1% of cells showed positive CD163 staining. This suggests that most macrophages in Patient 5 had the features of M1 macrophages. Our results may indicate that high  $^{18}\text{F}$ -FSPG uptake might represent an active disease state that is detectable by measuring xCT transporter activity in activated M1 macrophages. M1 and M2 macrophages appear to be opposing in nature such as proinflammatory vs. anti-inflammatory (13). Our results suggest a potential usefulness of  $^{18}\text{F}$ -FSPG PET in



differentiating macrophage polarization. Our IHC results may also explain why  $^{18}\text{F}$ -FSPG uptake was negligible 3 days after turpentine oil injection into the calf muscle (9).

The biodistribution of  $^{18}\text{F}$ -FSPG here is consistent with previously reported data in cancer patients (10). Especially, the low background would be very advantageous in detecting inflammatory/infectious lesions, especially in the brain, heart, and intestine where the application of  $^{18}\text{F}$ -FDG is limited because of normal physiological uptake.

There are several limitations in this study. The detection rate must be considered with caution because of the small number of patients. Furthermore, most patients had pulmonary diseases. IHC analysis is limited by the small amount of tissue available. Therefore, the current data are too limited to draw any firm conclusions from the IHC results.

## **CONCLUSION**

$^{18}\text{F}$ -FSPG PET may detect inflammatory lesions where activated macrophages/monocytes are present such as in sarcoidosis. Further studies in a larger number of patients should be performed to validate whether  $^{18}\text{F}$ -FSPG PET can detect inflammatory/infectious foci in relation to disease activity in a greater variety of inflammatory/infectious diseases and from different body locations.

## **DISCLOSURE**

S. J. Oh and D. H. Moon received a research grant from Piramal Imaging GmbH. N Koglin, A. Stephens and L. M. Dinkelborg were employed by Piramal Imaging GmbH. N. Koglin has ownership interests in Patents covering the applications of  $^{18}\text{F}$ -FSPG. No other potential conflicts of interest relevant to this article are reported.

## **ACKNOWLEDGEMENTS**

This study was sponsored and financially supported by Bayer Pharma AG/Piramal Imaging GmbH, Berlin (Germany), and Korea Health Technology R&D Project through the Korea Health Industry Development Institute (KHIDI), funded by the Ministry of Health & Welfare, Republic of Korea (HI06C0868).

## REFERENCES

1. Lo M, Wang YZ, Gout PW. The x(c)- cystine/glutamate antiporter: a potential target for therapy of cancer and other diseases. *J Cell Physiol.* 2008;215:593-602.
2. Sato H, Fujiwara K, Sagara J, Bannai S. Induction of cystine transport activity in mouse peritoneal macrophages by bacterial lipopolysaccharide. *Biochem J.* 1995;310 ( Pt 2):547-551.
3. Nabeyama A, Kurita A, Asano K, et al. xCT deficiency accelerates chemically induced tumorigenesis. *Proc Natl Acad Sci U S A.* 2010;107:6436-6441.
4. Lewerenz J, Hewett SJ, Huang Y, et al. The cystine/glutamate antiporter system x(c)(-) in health and disease: from molecular mechanisms to novel therapeutic opportunities. *Antioxid Redox Signal.* 2013;18:522-555.
5. Edinger AL, Thompson CB. Antigen-presenting cells control T cell proliferation by regulating amino acid availability. *Proc Natl Acad Sci U S A.* 2002;99:1107-1109.
6. Angelini G, Gardella S, Ardy M, et al. Antigen-presenting dendritic cells provide the reducing extracellular microenvironment required for T lymphocyte activation. *Proc Natl Acad Sci U S A.* 2002;99:1491-1496.
7. Vene R, Delfino L, Castellani P, et al. Redox remodeling allows and controls B-cell activation and differentiation. *Antioxid Redox Signal.* 2010;13:1145-1155.
8. Kim JY, Kanai Y, Chairoungdua A, et al. Human cystine/glutamate transporter: cDNA cloning and upregulation by oxidative stress in glioma cells. *Biochim Biophys Acta.* 2001;1512:335-344.
9. Koglin N, Mueller A, Berndt M, et al. Specific PET imaging of xC- transporter activity using a (1)(8)F-labeled glutamate derivative reveals a dominant pathway in tumor metabolism. *Clin Cancer Res.* 2011;17:6000-6011.
10. Baek S, Choi CM, Ahn SH, et al. Exploratory clinical trial of (4S)-4-(3-[18F]fluoropropyl)-L-glutamate for imaging xC- transporter using positron emission tomography in patients with non-small cell lung or breast cancer. *Clin Cancer Res.* 2012;18:5427-5437.
11. Valeyre D, Prasse A, Nunes H, Uzunhan Y, Brillet PY, Muller-Quernheim J. Sarcoidosis. *Lancet.* 2014;383:1155-1167.
12. Murray PJ, Allen JE, Biswas SK, et al. Macrophage activation and polarization: nomenclature and experimental guidelines. *Immunity.* 2014;41:14-20.
13. Stout RD, Suttles J. Functional plasticity of macrophages: reversible adaptation to changing microenvironments. *J Leukoc Biol.* 2004;76:509-513.

## FIGURE LEGENDS

**FIGURE 1.** A 53-y-old male with sarcoidosis (Patient 5).  $^{18}\text{F}$ -FDG (A) and  $^{18}\text{F}$ -FSPG (B) present similar major uptakes involving pleura, supraclavicular, and thoracic lymph nodes. The only differences are normal physiologic uptakes in brain, pancreas, and kidney. On IHC evaluation, the proportion of inflammatory cells positive for xCT (C), CD44 (D), CD68 (E), and CD163 (F) were 80%, 80%, 80%, and 1% (x400 magnification), respectively.

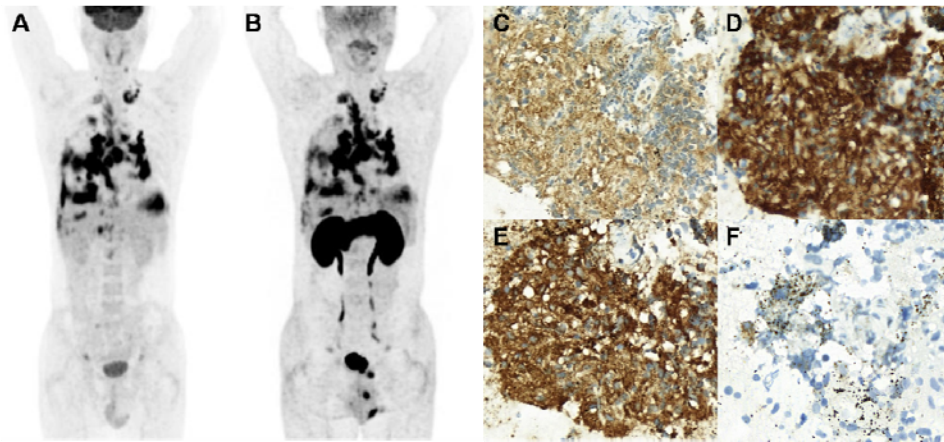


**FIGURE 2.**  $^{18}\text{F}$ -FSPG and  $^{18}\text{F}$ -FDG uptake in reference lesions at 60 minutes post-injection. There was no significant difference in SUVR between  $^{18}\text{F}$ -FSPG and  $^{18}\text{F}$ -FDG in sarcoidosis (A), but it was significantly lower in non-sarcoidosis (A). The SUVmax value of  $^{18}\text{F}$ -FSPG was significantly lower than those of  $^{18}\text{F}$ -FDG in both sarcoidosis and non-sarcoidosis (B).

